Probabilistic Performance-Based Optimum Seismic Design Framework: Illustration and Validation

Yong Li[1, *], Joel P. Conte[2] and Philip E. Gill[3]

Abstract: In the field of earthquake engineering, the advent of the performance-based design philosophy, together with the highly uncertain nature of earthquake ground excitations to structures, has brought probabilistic performance-based design to the forefront of seismic design. In order to design structures that explicitly satisfy probabilistic performance criteria, a probabilistic performance-based optimum seismic design (PPBOSD) framework is proposed in this paper by extending the state-of-the-art performance-based earthquake engineering (PBEE) methodology. PBEE is traditionally used for risk evaluation of existing or newly designed structural systems, thus referred to herein as forward PBEE analysis. In contrast, its use for design purposes is limited because design is essentially a more challenging inverse problem. To address this challenge, a decision-making layer is wrapped around the forward PBEE analysis procedure for computer-aided optimum structural design/retrofit accounting for various sources of uncertainty. In this paper, the framework is illustrated and validated using a proof-of-concept problem, namely tuning a simplified nonlinear inelastic single-degree-of-freedom (SDOF) model of a bridge to achieve a target probabilistic loss hazard curve. For this purpose, first the forward PBEE analysis is presented in conjunction with the multilayer Monte Carlo simulation method to estimate the total loss hazard curve efficiently, followed by a sensitivity study to investigate the effects of system (design) parameters on the probabilistic seismic performance of the bridge. The proposed PPBOSD framework is validated by successfully tuning the system parameters of the structure rated for a target probabilistic seismic loss hazard curve. The PPBOSD framework provides a tool that is essential to develop, calibrate and validate simplified probabilistic performance-based design procedures.

Keywords: Performance-based seismic design, optimum seismic design, forward PBEE analysis, inverse PBEE analysis, uncertainty quantification, hazard deaggregation.

[1] Department of Civil and Environmental Engineering, University of Alberta, Edmonton, AB T6G 1H9, Canada.

[2] Department of Structural Engineering, University of California, San Diego, 9500 Gilman Drive, La Jolla, CA 92093, USA.

[3] Department of Mathematics, University of California, San Diego, 9500 Gilman Drive, La Jolla, CA 92093, USA.

[*] Corresponding Author: Yong Li. Email: yong9@ualberta.ca.

1 Introduction

The seismic design philosophy has evolved from the safeguard against collapse of structures and loss of life to performance-based seismic design (PBSD). Aimed at improving and ensuring post-earthquake functionality, PBSD has been developed in response to the substantial economic losses due to earthquakes (e.g., a total loss of $24 billion for the 1994 Mw 6.7 Northridge earthquake [Eguchi, Goltz, Taylor et al. (1998)]. However, uncertain structural performance is inevitable because of various sources of uncertainty, i.e., the randomness in structural loads (e.g., earthquake loads), the variability in demands imposed on the structural system, and the uncertainties in the capacity of the system to withstand those demands as well as other socio-economic variables (e.g., uncertainty in repair cost for damaged components). With the highly uncertain nature of earthquake ground motions, the advent of performance-based design philosophy has brought probabilistic PBSD to the forefront of seismic design. The need to account for these uncertainties has prompted the development of a modular probabilistic performance evaluation methodology, the performance-based earthquake engineering (PBEE) methodology, under the auspice of the Pacific Earthquake Engineering Research (PEER) Center [Cornell and Krawinkler (2000)]. PBEE aims to evaluate probabilistically the seismic performance of a structure under specific site and soil conditions in an uncertainty propagation framework, herein referred to as forward PBEE analysis. In the last two decades, significant research efforts have been devoted to the development of the PEER PBEE methodology [Cornell and Krawinkler (2000); Porter (2003); Baker (2007); Günay and Mosalam (2013); Lin, Haselton and Baker (2013)]. Applications of the PEER PBEE methodology for probabilistic performance assessment of various testbed structures can be found in the literature [Comerio (2005); Kunnath, Larson and Miranda (2006); Zhang (2006); Conte and Zhang (2007); Goulet, Haselton, Mitrani-Reiser et al. (2007); Haselton, Liel, Deierlein et al. (2011); Mosalam and Günay (2014); Li and Conte (2017); Romano, Faggella, Gigliotti et al. (2018); Li and Conte (2019)]. With its wide acceptance as a tool for probabilistic performance assessment, the PEER PBEE methodology has formed the basis for structural design codes or evaluation guidelines, e.g., FEMA P-58 [FEMA (2012)] in which PBEE is specialized to performance-based seismic assessment of new and existing building structures.

Notwithstanding the significant progress in PBEE for probabilistic performance assessment, more limited research has been performed in inverse PBEE for structural design purposes [Jalayer and Cornell (2003); Mackie and Stojadinovic (2007); Zakeri and Zareian (2017)]. This is due to the probabilistic nature of the PBEE methodology, which hinders its application to the design process to achieve a design target explicitly described in probabilistic terms. The design process is essentially a decision-making process. Old-fashioned design was performed through a manual trial-and-error approach, guided by a both a simple design philosophy and engineering experience. Currently, in professional practice, the uncertainties are accounted for by applying a subjective "factor of safety approach" in the allowable stress methodology or a semi-probabilistic "partial safety approach" in the Load and Resistance Factor Design (LRFD) [Ellingwood (2000)]. The application of a fully probabilistic and risk-informed approach (e.g., PBEE) in developing a practical performance-based design methodology requires the inversion of the available

probabilistic performance-based assessment methodology, herein referred to as the inverse PBEE analysis. In order to conquer the inverse problem of explicitly satisfying probabilistic performance criteria confronted in the design process, computer-aided structural design using mathematical optimization becomes essential because of the increased complexity in the probabilistic design process [Austin, Pister and Mahin (1987); Haukaas (2008)].

It is worth noting that significant research has been performed on a closely related topic, i.e., reliability-based seismic design optimization [Jensen, Valdebenito, Schuëller et al. (2009); Taflanidis and Beck (2009); Barbato and Tubaldi (2013); Tubaldi, Barbato and Dall'Asta (2016)], which also addresses the inverse problem in the presence of uncertainties. In these studies, the seismic design problem is treated as an inverse problem considering uncertainties associated with the earthquake loading (intensity and time history) and in some cases the structural model parameters. The inverse problem was cast either as a zero-finding problem [Barbato and Tubaldi (2013)] to achieve a target reliability, or as an optimization problem, in which reliability metrics (i.e., the probability of failure of the system) are used to define the objective/constraint functions. However, these studies focused on the system reliability (or probability of failure) based on a pre-defined critical threshold value of a response quantity, instead of the full probabilistic description of the structural system performance at a continuum of levels of response (demand) and loss and at a discrete set of damage states. It is also worth mentioning that the above studies represent the earthquake ground motions analytically as a random process (e.g., non-stationary filtered white noise process) linked to a ground motion intensity measure such as the peak ground acceleration (PGA). In contrast, the study reported in this paper uses ensembles of scaled historic earthquake ground motion records to represent the record-to-record variability in the forward PBEE analysis. These earthquake records are selected based on the magnitude-distance deaggregation of the site seismic hazard, the geological and seismological conditions and the local site conditions. This earthquake ground motion characterization is currently predominantly used in performance-based earthquake engineering, both at the level of research and engineering practice.

The aforementioned need calls for an innovative optimum seismic design framework in the presence of uncertainty by using the versatile and modular probabilistic PBEE methodology. Aiming at promoting the practical application of probabilistic methods for design purposes, this paper proposes a probabilistic performance-based optimum seismic design (PPBOSD) framework. This framework is an extension of the PBEE methodology obtained by wrapping a decision-making layer in the design process around the forward PBEE analysis using mathematical optimization. The PPBOSD framework is illustrated and validated using a simplified nonlinear inelastic single-degree-of-freedom (SDOF) model of a bridge structure as a proof-of-concept study, before applying it to more complex and realistic engineering problems in the future. In the validation example, a well-posed optimization problem of tuning system (design) parameters of the structure to achieve a target probabilistic loss hazard curve is defined and solved using the proposed PPBOSD framework.

This paper is structured as follows. First, the motivation behind the proposed PPBOSD framework is articulated, and an illustrative example of a SDOF bridge model, which is used to demonstrate conceptually the application of the PPBOSD framework, is presented.

Second, the steps of the forward PBEE analysis, which is an indispensable component of PPBOSD, are described in the context of quantitatively assessing the seismic performance of the illustrative structure in probabilistic terms. Note that a multilayer Monte Carlo simulation procedure is implemented to estimate efficiently the total seismic loss hazard of the structure, which is needed in the PPBOSD framework. Third, a parametric probabilistic PBEE analysis is conducted to investigate the effects of the system (design) parameters on the probabilistic seismic performance of the structure. Finally, for illustration and validation purposes, the inelastic SDOF bridge model parameters are optimized (i.e., tuned), using the PPBOSD framework, to achieve a target seismic loss hazard curve of the bridge. The underlying assumptions and limitations of the presented research are critically discussed in the conclusions.

2 PPBOSD framework and illustrative application

The well-established PEER PBEE methodology is used primarily to sequentially quantify and analyze the uncertainties in the seismic intensity and earthquake records, structural response (demand), structural capacity, seismic damage (i.e., limit-state exceedances), and eventually the seismic loss (e.g., repair cost, down time) for a structure, at a given site, due to future earthquakes. The PBEE methodology (i.e., forward PBEE analysis) consists of four analytical steps: probabilistic seismic hazard analysis, probabilistic demand hazard analysis, probabilistic damage hazard analysis, and probabilistic loss hazard analysis (Fig. 1). Each step determines the probabilistic characteristics of intermediate (or interface) variables, respectively referred to as the earthquake ground motion Intensity Measure (IM), Engineering Demand Parameter (EDP), Damage Measure (DM), and Decision Variable (DV) such as monetary loss.
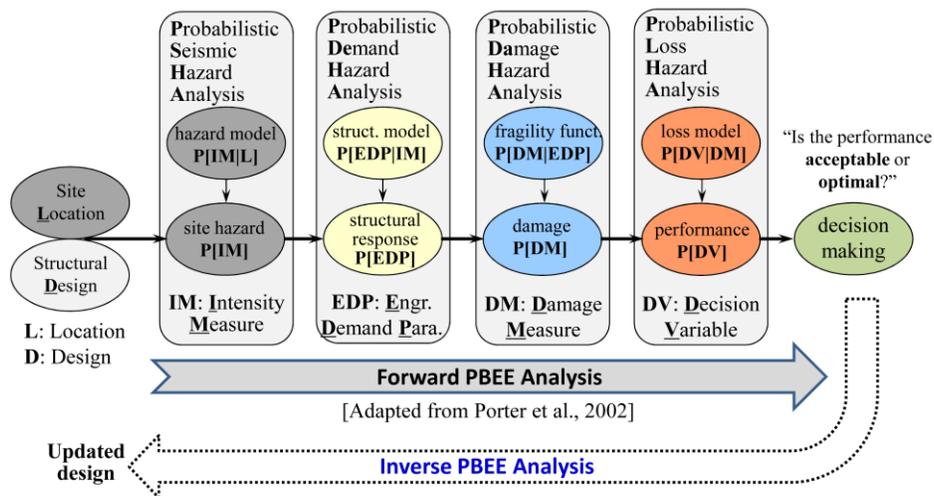
Figure 1: Forward PBEE analysis and need for inverse PBEE analysis

For a newly designed or an existing structure, forward PBEE analysis can be used as a reliable tool to assess its probabilistic seismic performance, which depends on the system parameter vector **x** consisting of geometric, material and mechanical properties of the

various structural components and seismic mitigation devices of the structure. However, the probabilistic performance of the structure may be unacceptable or not optimal according to target seismic design objectives, which are typically defined, based on the public's expectations, by stakeholders, decision-makers and design code committees. This underlies the motivation behind an inverse PBEE analysis. For example, through the evaluation process using PBEE, an initial structural design is characterized by its seismic demand or loss hazard curve (i.e., probability of exceedance of any specified value of EDP or DV in 100 years) such as the hazard curve #1 in Fig. 2 expressed in terms of the probability of exceedance in 100 years. In contrast, the target performance can be characterized by hazard curve #2, #3, or #4 which would require tuning the design parameter vector **x** for this target design specification. Ideally, it is desirable to reduce the seismic risk (i.e., probability of exceedance) across the entire range of EDP or DV values, e.g., from hazard curve #1 to hazard curve #4. However, if hazard curve #4 is not feasible due to practical design constraints such as the initial construction cost, the decision-makers (e.g., engineers, stakeholders, or owners) can aim at improving the design by targeting hazard curve # 2 or hazard curve #3 as an alternative to reducing the seismic risk across all EDP or DV values. Namely, the decisions are made to place more emphasis in the seismic performance either at the low hazard level (or short return period or high probability of exceedance) or at the high hazard level (or long return period or low probability of exceedance), respectively.
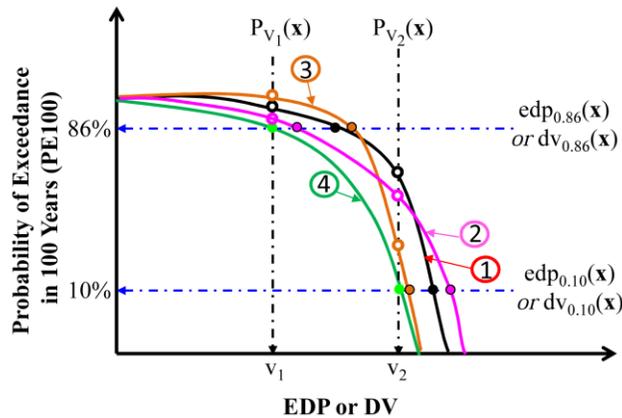
Figure 2: Illustration of the motivation for proposed probabilistic performance-based optimum seismic design framework

When aiming at improving the seismic performance at low hazard (or short return period or high probability of exceedance) levels, the performance of the initial structural design can be improved from hazard curve #1 to hazard curve #2. As seen from Fig. 2, this can be achieved by either minimizing the probability, $P_{V_1}(\mathbf{x})$, of exceeding a low threshold value v_1 of the EDP or DV, or by minimizing the 86th percentile of the EDP ($edp_{0.86}$) or DV ($dv_{0.86}$), both of which may lower the structural performance at high hazard levels (or long return period or low probability of exceedance). Conversely, improving the seismic performance at high hazard levels may reduce the performance at low hazard levels. In

such a case, for example, the initial structural design could be altered so that its performance characterized by hazard curve #1 is improved to the performance characterized by hazard curve #3. Similarly, this can be achieved by either minimizing the probability, $P_{v_2}(\mathbf{x})$, of exceeding a high threshold value v_2 of the EDP or DV or by minimizing the 10th percentile of the EDP ($edp_{0.10}$) or DV($dv_{0.10}$) (see Fig. 2). Note that 10% (a high hazard level) and 86% (a low hazard level) probability of exceedance in 100 years correspond to return periods of 945 years and 50 years, respectively, based on the assumption of the Poisson random occurrence model. Alternatively, and more generally, the complete target loss hazard curve (defined by many discrete points at different hazard levels) can be used to express the probabilistic design objectives, as shown later in the illustrative example.

The above inverse PBEE problem, which is confronted for design improvement or design optimization in the face of uncertainty, can be solved by the innovative optimum structural design framework (i.e., PPBOSD) proposed in this paper. PPBOSD extends the PBEE evaluation methodology, which can be viewed as an open loop, by wrapping a decision-making layer using optimization around the forward PBEE analysis in order to close the loop as shown in Fig. 3. This decision-making layer allows the use of various computational optimization tools, e.g., *OpenSees-SNOPT* [Gu, Barbato, Conte et al. (2012)], to update the initial structural design to achieve the performance objectives. The probabilistic seismic design objectives can be defined in terms of demand hazard, damage hazard, and/or loss hazard characteristics (e.g., hazard curves of EDP or DV, probability of limit-state exceedances, or statistics of EDP, DM, and/or DV in a specified exposure time). These design objectives can be cast into either objective or constraint functions in the optimization problem formulation. Thus, the proposed PPBOSD framework provides a tool to search for either a feasible design that satisfies all constraint functions or an optimum design that minimizes the objective function while satisfying all constraint functions. In PPBOSD, the current design is first assessed using the forward PBEE analysis for its probabilistic performance, which is compared with the design objectives expressed in terms of target hazard levels or statistics. If the design objectives are not satisfied, the current design will be updated in the decision-making layer through optimization by tuning the structural design parameters $\mathbf{x}$.

This paper focuses on the illustration and validation of the proposed PPBOSD framework, rather than a practical application to a complex large-scale bridge system, which is considered as the next stage of this research. Accordingly, a simple nonlinear bridge structural model is selected herein for simplicity but without loss of generality. This structural model consists of an inelastic SDOF system, which is commonly used to represent macroscopically a bridge behavior in its longitudinal or transverse direction. A nonlinear FE model of the Humboldt Bay Middle Channel Bridge (HBMC, see Fig. 4(a)) previously developed in *OpenSees* [Conte and Zhang (2007)] is used to calibrate the nonlinear SDOF system parameters. The initial stiffness of the SDOF model obtained from the static pushover analysis of the bridge in the longitudinal direction is k_0=137,200 kN/m, and the effective lumped mass accounted for is m=6.15×10⁶ kg, thus leading to an initial fundamental period of vibration T_1=1.33 s. The nonlinear model parameters associated with this inelastic SDOF model (Fig. 4(b)) are the yield strength F_y=10,290 kN

(i.e., corresponding to a yield displacement U_y=0.075 m), and the post-yield stiffness ratio (=ratio of the post-yield stiffness to the initial stiffness) b=0.10. The *Menegotto-Pinto* hysteretic material model is used to approximately represent the cyclic force-displacement response behavior and energy dissipation capabilities of an inelastic structural system such as a bridge. Furthermore, linear viscous damping with a damping ratio of 2% is incorporated in the SDOF bridge model to account for sources of energy dissipation beyond the hysteretic energy dissipation due to inelastic action of the materials during an earthquake. Note that the nonlinear SDOF bridge model is used in this study only for the purpose of illustrating and validating the proposed PPBOSD framework, these being the main objectives of this paper, without the intention to assess comprehensively the probabilistic seismic performance of the actual bridge.
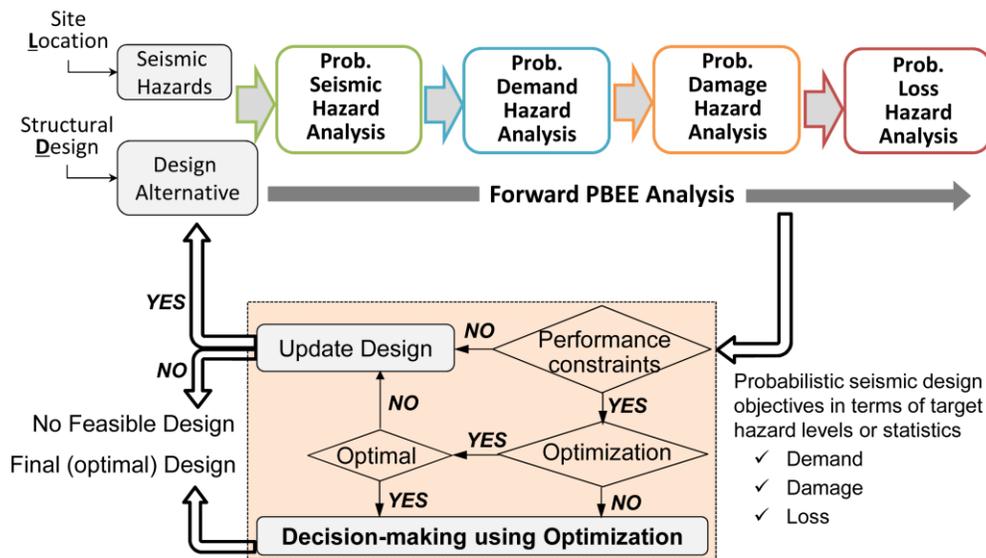
Figure 3: Probabilistic performance-based optimum seismic design (PPBOSD) framework

(a)   (b)

Figure 4: Humboldt bay middle channel (HBMC) bridge (courtesy of Caltrans): (a) isometric view, and (b) simplified nonlinear SDOF model to represent the longitudinal nonlinear response behavior of the bridge

In engineering practice, various structural response quantities or parameters, referred to as engineering demand parameters (EDPs), strongly correlated with different types of structural or non-structural damage are of interest. This study considers three EDPs, namely relative displacement ductility, μ , peak absolute acceleration, $A_{Abs.}$, and normalized hysteretic energy dissipated, E_H, as defined in Eqs. (1)-(3), respectively.

$$\mu = \underset{0 < t < t_d}{Max} \left(\frac{|u(t)|}{U_y} \right) \tag{1}$$

$$A_{Abs.} = \underset{0 < t < t_d}{Max} \left(\frac{|\ddot{u}(t) + \ddot{u}_g(t)|}{g} \right) \tag{2}$$

$$E_H = \frac{\int_0^{t_d} R(t)\,du(t) - E_E(t_d)}{F_y U_y} \tag{3}$$

In the equations above, t_d =earthquake duration (i.e., the total duration of the ground motion record downloaded from the PEER NGA database), $u(t)$ =displacement response relative to the ground, $\ddot{u}(t)$ =relative acceleration response, $\ddot{u}_g(t)$ =earthquake ground acceleration, g =acceleration due to gravity, $R(t)$ =internal resisting force, and $E_E(t_d)$ =elastic strain energy stored in the system at time $t = t_d$. The three response parameters defined in Eqs. (1)-(3) are selected as EDPs associated with the following damage/failure or limit-states: first-excursion failure, dynamic stability of vehicles traversing the bridge during the earthquake, and cumulative damage (e.g., low-cycle fatigue damage), respectively.

3 Forward PBEE analysis

The PEER PBEE methodology breaks down the seismic risk assessment procedure into four successive steps. These probabilistic steps sequentially quantify the uncertainty in the earthquake ground motion intensity measure (IM), the engineering demand parameter (EDP), the damage measure (DM) and the decision variable (DV), as implied by the underlying mathematical model expressed in Eq. (4).

$$\nu_{DV}(dv) = \iiint G(dv \mid dm, edp, im) \cdot |G(dm \mid edp, im)| \cdot |dG(edp \mid im)| \cdot |d\nu_{IM}(im)| \tag{4}$$

Here, $\nu_X(x)$ denotes the mean annual rate (MAR) of occurrence of the random event $\{X > x\}$, namely the MAR of random variable X exceeding a given value x, and $G(x|y) = P(X > x|Y = y)$ represents the conditional complementary cumulative distribution function (CCDF) of random variable X given random variable $Y = y$. In the probabilistic conditioning and deconditioning process, "one-step" forward dependence is assumed, i.e., $G(dm|edp,im) = G(dm|edp)$ and $G(dv|dm,edp,im) = G(dv|dm)$. This

process aims at propagating the uncertainty related to the seismic input and structural capacity, all the way to the EDPs, DMs, and DVs using the total probability theorem. The four steps of the PEER PBEE methodology are described below with select results to illustrate the process of forward PBEE analysis, as well as deaggregation results to increase the transparency of the hazard analysis. A multilayer Monte Carlo simulation method [Zhang (2006); Yang, Moehle, Stojadinovic et al. (2009)] is implemented to estimate efficiently the total loss hazard of the structure.

3.1 Probabilistic seismic hazard analysis

Pioneered by the theoretical framework developed by Cornell [Cornell (1968)], probabilistic seismic hazard analysis (PSHA), Step (1) of the PBEE methodology, has become the most accepted approach for assessing the site-specific seismic hazard in a probabilistic manner [Shome, Cornell, Bazzurro et al. (1998); Luco and Cornell (2007); Petersen, Frankel, Harmsen et al. (2008)]. The probabilistic seismic hazard, which consists of the uncertainty quantification of the earthquake ground motion IM, is characterized by the MAR of the earthquake ground motion IM exceeding a specified threshold value im, $\nu_{IM}(im) = \nu_{IM}(IM > im)$. Based on the Poisson process assumption for the random occurrence of earthquakes in time, the MAR of exceedance can be converted to the probability of exceedance (PE) in a specified exposure time (e.g., annual PE or PE in 50 years abbreviated as PE50). The IM is selected as the 5% damped linear elastic pseudo-spectral acceleration at the fundamental period (T_1) of the structural system $S_a(T_1, \xi = 5\%)$, which has been shown to be a statistically efficient and sufficient predictor among a family of earthquake ground motion intensity measures [Shome, Cornell, Bazzurro et al. (1998); Luco and Cornel (2007)].

The PSHA for a specific site location and soil condition can be performed using the 2008 Interactive Deaggregation tool provided by the United States Geological Survey (USGS). The site location in this study is assumed to be in the City of Oakland, California, at latitude=37.803° N and longitude=122.287° W. The soil condition is characterized by the average shear wave velocity in the top 30 meters of soil at the site location (V_{s30}=360 m/s). The seismic hazard curve obtained from the 2008 Interactive Deaggregation tool will be needed in Step (2) of the forward PBEE analysis.

The seismic hazard can be deaggregated with respect to the seismological variables, i.e., magnitude (M) and source-to-site distance (R), to gain additional insight into the contributing earthquakes. This insight will benefit the earthquake ground motion selection for the ensemble time history analyses. Fig. 5 shows the M-R deaggregation of the seismic hazard corresponding to PE50=2%, and two modes are observed in the M-R plane. The higher mode is mainly contributed by the Hayward Fault to the east of Oakland, and the lower mode is mainly contributed by the San Andreas Fault to the west of Oakland. This deaggregation information (i.e., 5.9<M<7.3 corresponding to the primary mode, 0<R<40 km) guided the earthquake ground motion selection process, together with the geological and seismological conditions (i.e., fault mechanism as strike-slip) and local site conditions. Accordingly, a large number (i.e., 146) of horizontal earthquake ground motion records are selected from the PEER NGA database of

historical records, and are used as seismic inputs for the ensemble nonlinear time history analyses required for the probabilistic characterization of the seismic response (or demand) in the second step of the PBEE analysis.
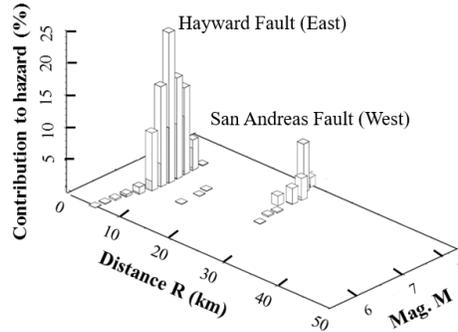
Figure 5: M-R deaggregation of the probabilistic seismic hazard corresponding to a probability of exceedance of 2% in 50 years (PE50=2%)

3.2 Probabilistic demand hazard analysis

Probabilistic demand hazard analysis (PDeHA) aims at predicting probabilistically the structural response (i.e., EDP) to future earthquakes. The probabilistic characterization of an EDP is obtained through the corresponding seismic demand hazard curve, which is defined as the MAR of *EDP* exceeding a threshold value *edp*, $\nu_{EDP}(edp)$, or alternatively the probability of exceedance in 50 years, $PE50 = P[EDP > edp]$ in an exposure time of 50 years. Mathematically, through the total probability theorem, the demand hazard curve is obtained as the convolution of $P[EDP > edp|IM = im]$, the conditional CCDF of the *EDP* given $IM = im$, and the demand hazard curve $\nu_{IM}(im)$, thus accounting for all seismic hazard levels, as

$$\nu_{EDP}(edp) = \int_{IM} P[EDP > edp|IM = im]|d\nu_{IM}(im)| \tag{5}$$

Thus, a crucial step of probabilistic demand hazard analysis is to find the probability distribution of the EDP of interest given a value *im* of *IM*, $P[EDP > edp|IM = im]$, which is referred to as the probabilistic demand conditional on the seismic hazard level. The conditional probabilistic demand analysis can be performed through the commonly used cloud method [Baker (2005)]. In this method, an ensemble of nonlinear dynamic analyses of the structure of interest are performed for the selected suite of earthquake ground motion records, which have various IM values. The corresponding seismic response dataset for the selected earthquakes, $[im_i, edp_i]$ ($i = 1, 2, \cdots, 146$), is used to build a statistical model of *EDP* given *IM* based on linear regression analysis. The conditional mean value of $\ln EDP$ given *IM*, $\mu_{\ln EDP|IM}$, is estimated as

$$\hat{\mu}_{\ln EDP|IM} = \hat{a} + \hat{b} \ln IM \tag{6}$$

and the conditional variance, $\sigma^2_{\ln EDP|IM}$, is estimated as

$$\hat{s}^2 = \frac{\sum_{i=1}^{n} \left[\ln edp_i - \left(\hat{a} + \hat{b} \ln im_i \right) \right]^2}{n-2} \tag{7}$$

where $\hat{a}$ and $\hat{b}$ are obtained through regression analysis. Accordingly, the conditional random variable $\{EDP \mid IM = im\}$ is fully characterized by the conditional probability density function (PDF) (see Fig. 6) or conditional CCDF, $G_{EDP|IM}(edp \mid im)$, which often, including for the example presented here, is well represented by the lognormal probability distribution,

$$G_{EDP|IM}(edp \mid im) = P[EDP > edp \mid IM = im] = 1 - \Phi \left[\frac{\ln edp - \left(\hat{a} + \hat{b} \ln im \right)}{\hat{s}} \right] \tag{8}$$

where Φ is the standard normal CDF and ln denotes the natural logarithmic function.
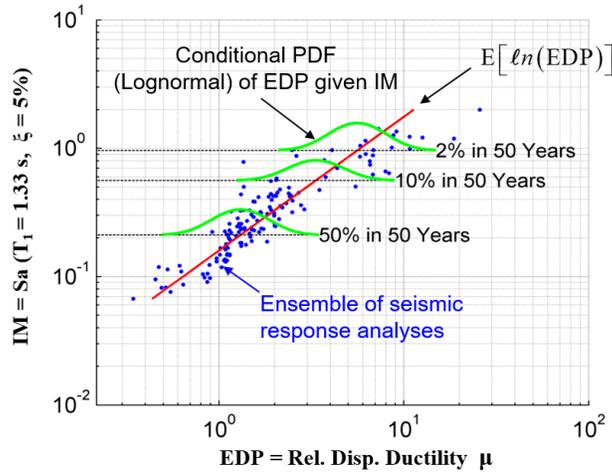
Figure 6: Conditional seismic demand hazard analysis result for EDP=relative displacement ductility

The conditional probabilistic demand reflects the record-to-record variability when the earthquake IM is fixed. To account for the uncertainty in the earthquake IM, the convolution of the conditional CCDF of the EDP and the seismic hazard curve obtained through PSHA is performed according to Eq. (6). This leads to the (unconditional) probabilistic demand hazard curve, $v_{EDP}(edp)$, as shown in Fig. 7(a) for EDP=relative displacement ductility (μ). The demand hazard curve presented shows that the MAR of the relative displacement ductility exceeding $\mu = 1, 2, 4, 6, 8$ is 1.84×10^{-2}, 0.77×10^{-2},

0.16×10^{-2}, 0.04×10^{-2}, and 0.01×10^{-2}, respectively, as indicated by the solid circles in Fig. 7(a). Note that the MAR of exceedance of 1.84×10^{-2} corresponds to a mean return period of 55 years ($=1/1.84\times10^{-2}$), i.e., the relative displacement ductility will exceed 1.0 (i.e., the structure will yield) at least once every 55 years on average.

The seismic demand hazard with a given MAR of exceedance arises from a continuous range of seismic hazard levels (or IM values) as expressed by Eq. (6) and the contribution of each seismic hazard level to the demand hazard varies with the demand hazard level. In order to investigate the relative contribution of an IM bin (Δim_i) to a hazard point on the demand hazard curve, $\nu_{EDP}(edp)$, a demand hazard deaggregation analysis can be performed according to Eq. (9).

$$\nu_{EDP}(edp) = \int_{IM} P\left[EDP > edp | IM\right] \left|\frac{d\nu_{IM}(im)}{dim}\right| dim$$

$$\cong \sum_i P\left[EDP > edp | IM\right] \left|\frac{d\nu_{IM}(im_i)}{dim}\right| \cdot \Delta im_i$$

(9)

The right-hand term in the above equation is referred to as the deaggregation of the demand hazard (at *EDP=edp*) with respect to the intensity measure IM, indicating the contribution of the IM bin, Δim_i, to $\nu_{EDP}(edp)$. Fig. 7(b) shows the deaggregation results for the five seismic demand hazard points $(\mu=1, 2, 4, 6, 8)$ shown on the probabilistic seismic demand hazard curve in Fig. 7(a). The deaggregation curves shift towards higher IM values (i.e., to the right) as the EDP values increase, which reflects the fact that earthquake ground motions of higher intensity levels contribute more to higher values of the EDP. Similarly, the other two EDPs defined in Eqs. (2) and (3) are quantified probabilistically but not presented here due to space limitation [Li (2014)].
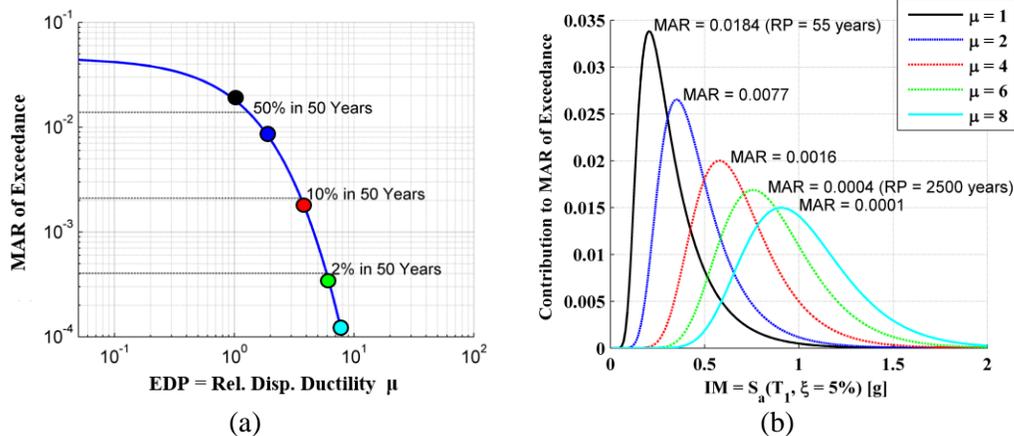
Figure 7: (a) Probabilistic seismic demand hazard curve for the relative displacement ductility (solid circles denoted for the points to be deaggregated), and (b) deaggregation of demand hazard points shown in Fig. 7(a) with respect to the intensity measure IM

3.3 Probabilistic damage hazard analysis

The third step of the PBEE methodology, probabilistic damage hazard analysis (PDaHA), is to predict probabilistically the seismic damage to the structure of interest due to future earthquakes. Practically, seismic damage is associated to a damage or failure mode (or mechanism). This study considers three damage or failure modes for the illustrative bridge structure, which are associated with the three selected EDPs, respectively. For each damage/failure mode/mechanism, a set of discrete limit-states are considered, corresponding to discrete values of the damage measure, $DM = k$. In this study, it is assumed that there are three limit-states $(n_{\text{limit-states}} = 3)$ for each damage/failure mode, i.e., $k \in (0, 1, 2, 3)$, corresponding to slight $(k = 1)$, moderate $(k = 2)$, and extensive $(k = 3)$ damage, respectively. Herein, the structure of interest is said to be in damage (or limit-) state DS_k if $\{DM = k\}$ and exceedance of the k-th damage (or limit-) state is denoted and defined as $EDS_k = \{DM \geq k\}$. The seismic damage hazard is characterized by the MAR, ν_{EDS_k}, of exceeding the k-th limit-state for each damage/failure mode. ν_{EDS_k} is computed through the convolution integral in Eq. (10),

$$\nu_{EDS_k} = \int_{EDP} P\big[DM \geq k \mid EDP = edp\big]\big|d\nu_{EDP}(edp)\big| \tag{10}$$

in which the conditional probability $P\big[DM \geq k \mid EDP = edp\big]$ is referred to in the literature as probabilistic capacity curve (or function) and characterizes the uncertainty in predicting the structural capacity against the k-th limit-state of the damage/failure mechanism of interest. Probabilistic capacity curves are typically obtained through comparing analytical or empirical capacity models with corresponding experimental data [Gardoni, Mosalam and Der Kiureghian (2002)]. For the purpose of this study, the probabilistic capacity curves for each of the three limit-states associated with each of the three damage/failure modes considered (first-excursion failure, dynamic stability of vehicles traversing the bridge, cumulative damage) are postulated (as normal CDFs) and defined in Tab. 1; they are also depicted graphically in Fig. 8(a).

The conditional probability of exceeding a damage (or limit-) state (e.g., $EDS_k = \{DM \geq k\}$), for a failure mode associated with a specific $EDP = edp$, $P\big[DM \geq k \mid EDP = edp\big]$, can be evaluated as $\sum_{dm \geq k} P\big[DM = dm \mid EDP = edp\big]$. The conditional probability of a damage state exceedance can then be convolved with the seismic demand hazard curve to yield the seismic damage hazard as in Eq. (10).

Fig. 8(b) reports the probability of exceeding damage or limit-states I, II, and III in 50 years for each of the three damage or failure modes considered, as well as the mean return periods (RPs) of damage/limit-state exceedances, which are commonly used to measure their occurrence frequency in engineering practice.

The seismic damage hazards calculated above contain contributions from a continuous range of EDP bins, as well as a continuous range of IM bins of the earthquake input

ground motions. Similar to the demand hazard deaggregation, the damage hazard can be deaggregated with respect to the associated EDP and the IM, respectively. Eqs. (11) and (12) show the contributions to the damage hazard v_{EDS_k} of the EDP bins, $\Delta(edp)_i$, and IM bins, $\Delta(im)_i$, respectively.

$$v_{EDS_k} \cong \sum_i P\left[DM > k \mid EDP = edp_i\right] \left|\frac{dv_{EDP}(edp_i)}{d(edp)}\right| \Delta(edp)_i \tag{11}$$

$$v_{EDS_k} \cong \int_{EDP} P\left[DM > k \mid EDP = \delta\right] \left|\int_{IM} dP\left[EDP > \delta \mid IM = im\right]\right| \frac{|dv_{IM}(im)|}{dim} dim$$

$$= \sum_i \sum_j P\left[DM > k \mid EDP = \delta_j\right] \left|dP\left[EDP > \delta_j \mid IM = im_i\right]\right| \frac{|dv_{IM}(im)|}{dim} \Delta im_i \tag{12}$$

Table 1: Parameters of postulated probabilistic capacity curves defined in terms of the normalized capacity (i.e., measured-to-predicted capacity ratios)

Associated EDP	Limit-States	Predicted capacity	Measured-to-predicted capacity ratio (Normally distributed)	
			Mean	**c.o.v**
Relative Displacement Ductility [-]	I	$\mu=2$	1.095	0.201
	II	$\mu=6$	1.124	0.208
	III	$\mu=8$	1.254	0.200
Peak Absolute Acceleration [g]	I	$A_{Abs}=0.10$	0.934	0.128
	II	$A_{Abs}=0.20$	0.952	0.246
	III	$A_{Abs}=0.25$	0.973	0.265
Normalized Hysteretic Energy Dissipated [-]	I	$E_H=5$	0.934	0.133
	II	$E_H=20$	0.965	0.140
	III	$E_H=30$	0.983	0.146
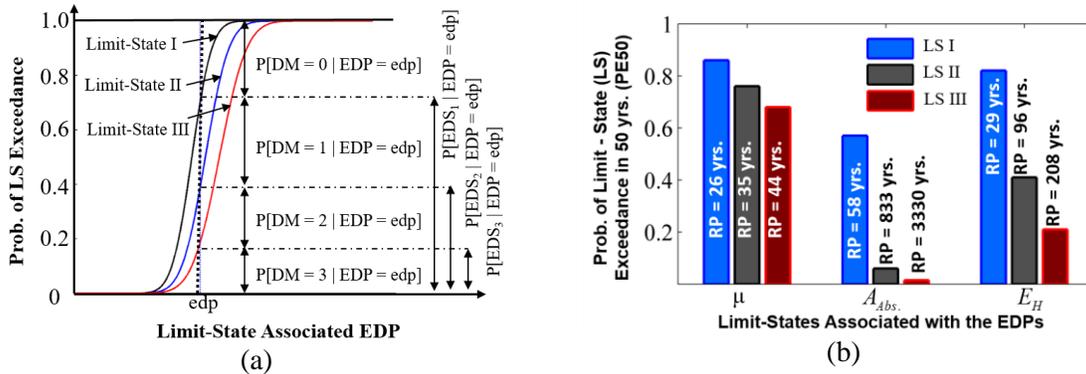
Figure 8: (a) Illustration of the probabilistic capacity curves and definition of conditional probability of damage states given EDP, and (b) seismic damage hazard results for the damage (or limit-) states associated with the EDPs considered for the illustrative example

The damage hazard deaggregation with respect to EDP and IM, shown in Fig. 9, reveals the relative contributions of different EDP or IM bins to the damage hazard. It shows that exceedance of increasingly severe damage/limit-states are predominantly contributed by increasing higher EDP or IM values or bins.
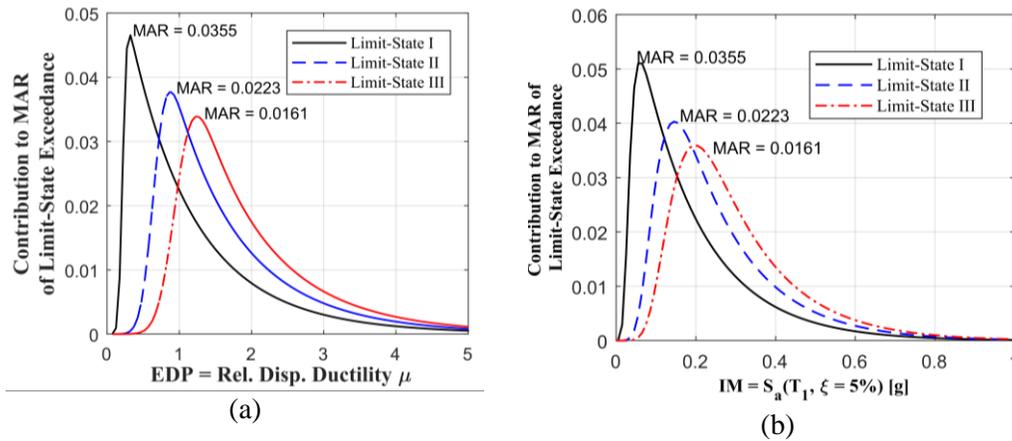
Figure 9: Damage hazard deaggregation with respect to (a) EDP and (b) IM for different damage/limit-state exceedances associated with EDP=relative displacement ductility (values of MAR of exceedance are indicated for each limit-state)

3.4 Probabilistic loss hazard analysis

The objective of the final step of the PBEE methodology, probabilistic loss hazard analysis (PLHA), is to quantify the decision variable (DV) probabilistically. The DV can be the direct economic loss (i.e., total repair or replacement cost, L_T) due to seismic damage, or the loss factor defined as the total loss normalized by the system replacement cost. The total loss hazard can be expressed in the form of a loss hazard curve, which provides the MAR or annual probability of the DV exceeding a threshold value. The total

loss L_T is defined as the summation of all the component-wise repair costs (L_j, j =1, 2, 3 here) associated with the three damage/failure modes considered here. In a real-world bridge application, which is more involved/detailed than the illustrative example considered here, the damage/failure modes would consist of: failure of bridge piers, failure of shear keys, failure of abutment, deck unseating, etc. In the present illustrative example, L_j is assumed to lump all the component-wise repair costs associated with the j-th damage/failure mechanism of the bridge. For each component, the loss hazard curve, $\nu_{L_j}(l)$, is obtained according to Eq. (13),

$$\nu_{L_j}(l) = \int_{DM} P\left[L_j > l \mid DM\right] \cdot \left|d\nu_{DM}\right| = \sum_{k=1}^{n_{\text{imit-states}}^{[j]}} P\left[L_j > l \mid DS_k^{[j]}\right] \cdot \left|\nu_{EDS_k^{[j]}} - \nu_{EDS_{k+1}^{[j]}}\right| \qquad (13)$$

in which the integration reduces to a summation over the discrete damage states (as favored in practice) considered for the j-th damage/failure mode. The repair cost conditional CCDF, $P\left[L_j > l \mid DS_k^{[j]}\right]$, quantifies the uncertainty in the component repair cost related to the j-th damage/failure mode given a damage level between the k-th and ($k+1$)-th limit-states (i.e., damage state $DS_k^{[j]}$). Due to lack of statistical data on repair and replacement costs, they are assumed to be normally distributed with the means and coefficients of variation (c.o.v.) presented in Tab. 2 to facilitate illustration of the methodology proposed in this paper.

Table 2: Statistics of repair costs as a function of failure mode and damage states

Failure mode associated EDP	Limit-State	Repair/Replacement cost	
		Mean ($)	c.o.v.
Relative Displacement Ductility [-]	I	146,500	0.12
	II	246,400	0.25
	III	350,000	0.32
Peak Absolute Acceleration [g]	I	55,000	0.11
	II	100,000	0.20
	III	500,000	0.28
Normalized Hysteretic Energy Dissipated [-]	I	55,650	0.13
	II	110,000	0.22
	III	520,000	0.28

With the probabilistic characteristics of the component losses determined in terms of component loss hazard, the total loss hazard can be computed through a multi-fold integration of the joint PDF of the component losses. However, it is computationally prohibitive, if not impossible, to derive that joint PDF and carry out the multi-fold integration, especially when a large number of components and damage/failure modes exist in real-world applications. To address this challenge, a multilayer Monte Carlo Simulation (MMCS) method is implemented and used as a simple yet powerful technique to estimate the total loss hazard. This method can efficiently incorporate and propagate the uncertainties arising at all stages of the PBEE analysis (e.g., random time occurrences of earthquakes governed by a Poisson process, IM, EDP, and DM) all the way to the final random variable DV=L_T. Such a treatment of uncertainty propagation in the forward PBEE analysis empowers the proposed PPBOSD framework, which involves a large number of forward PBEE analyses during the optimization process. The flowchart of the MMCS method developed for this study is shown in Fig. 10 and presented in detail below.

First, the number of earthquakes in the year being simulated is randomly generated according to the Poisson random occurrence model, and IM for each earthquake ground motion is simulated according to its probabilistic characteristics derived from PSHA. Second, for a given IM level, a set of EDPs is then stochastically simulated according to the joint PDF of the EDPs estimated through the results of an ensemble of FE seismic response analyses of the structure of interest. Note that the conditional joint PDF of the EDPs given IM can be approximated by a NATAF model [Liu and Der Kiureghian (1986)] defined by the marginal PDFs and correlation coefficients of the EDPs estimated from the results of the ensemble of nonlinear time-history analyses performed in the PSDeH analysis. This relaxes the more restrictive assumption, that the EDPs are jointly lognormal, used in FEMA P-58 and by Yang et al. [Yang, Moehle, Stojadinovic et al. (2009)]. Third, the damage measure for each component (or lump of components in the illustrative example presented here) is randomly generated from the probabilistic capacity curves, and the component loss is simulated according to the PDF of the corresponding repair cost. For each year simulated, the total loss for that year is obtained by summing the repair costs over all the damaged components and all the earthquakes that occurred during that year. By simulating the seismic activity and resulting structural damage and economic loss for a large number of years (e.g., 100,000), an empirical CDF and CCDF of the total loss can be obtained. The CCDF of the total loss is referred to as the seismic loss hazard curve.
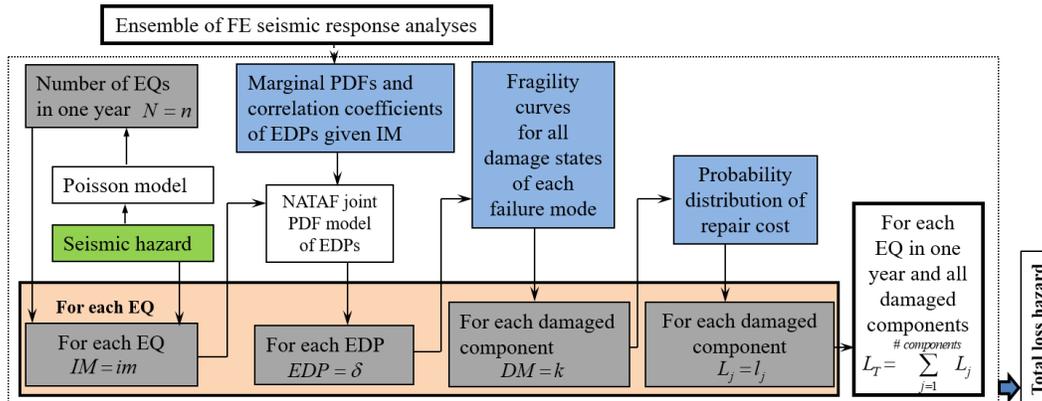
Figure 10: Flowchart of Multilayer Monte Carlo Simulation (MMCS) method for total loss hazard calculation

The seismic loss hazard curve shown in Fig. 11 for the bridge structure considered in this study was obtained using the MMCS method developed. The total loss hazard curve indicates the annual probability of the repair or replacement costs exceeding a threshold value. For example, from Fig. 11, there is 0.3% probability that for a given year, the seismic repair cost for this bridge will exceed 20% of the total bridge replacement cost (i.e., loss factor of 0.2) or, alternatively, this level of loss for the bridge has a mean return period of exceedance of 330 years (=1/0.003).
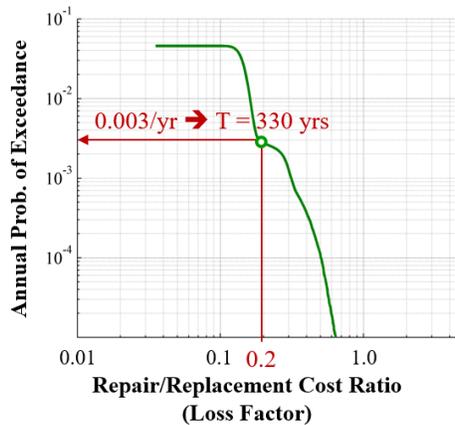
Figure 11: Probabilistic seismic loss hazard curve

4 Parametric forward PBEE analysis

Following the forward PBEE analysis procedure presented in the previous section, a parametric study (i.e., one-at-a-time perturbation-based sensitivity analysis) is performed in order to explore the effects of parametric changes on the forward PBEE analysis results. For the system considered in this paper, the yield strength (i.e., F_y) and the initial stiffness (i.e., k_0) of the nonlinear SDOF system are each perturbed by -25% and 50%. The effects of varying the yield strength on the demand hazard curves for the relative

displacement ductility and peak absolute deck acceleration are shown in Figs. 12(a) and 12(b), respectively. Note that an increase in the yield strength reduces the demand hazard for the relative displacement ductility, while it increases the demand hazard for the peak absolute deck acceleration. Consequently, varying the yield strength affects the loss hazard curve as well as shown in Fig. 13(a). By comparing Figs. 13(a) and 13(b), it is worth noting that the initial stiffness and the yield strength have opposite effects on the loss hazard curve.

The sensitivity study of the forward PBEE analysis results indicates that the loss hazard changes as a function of the system parameters, thus giving rise to an inverse PBEE problem. For example, it is of interest to the various stakeholders and owner of the structure of interest to tune the system design (i.e., design parameters) such that an expected performance, expressed in terms of a target or desired probabilistic loss hazard curve, is achieved.

(a) (b)
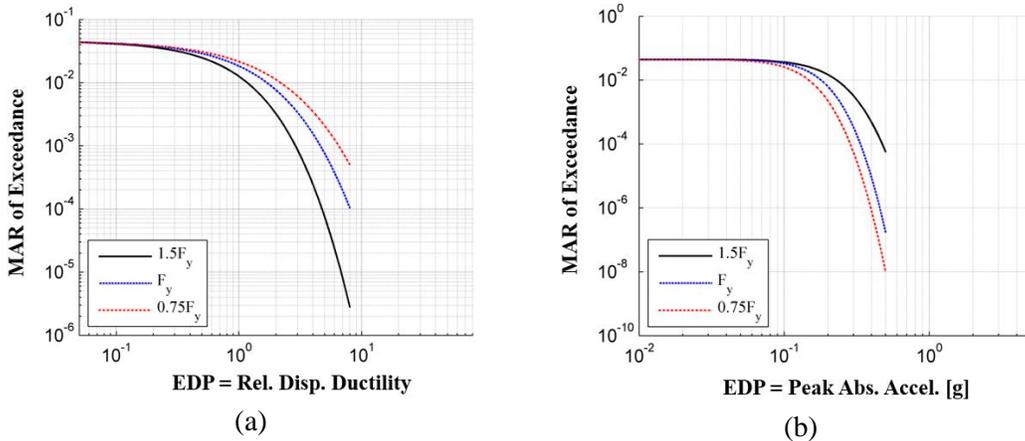
Figure 12: Probabilistic seismic demand hazard curves for: (a) relative displacement ductility, and (b) peak absolute acceleration of SDOF systems with different yield strengths

(a) (b)
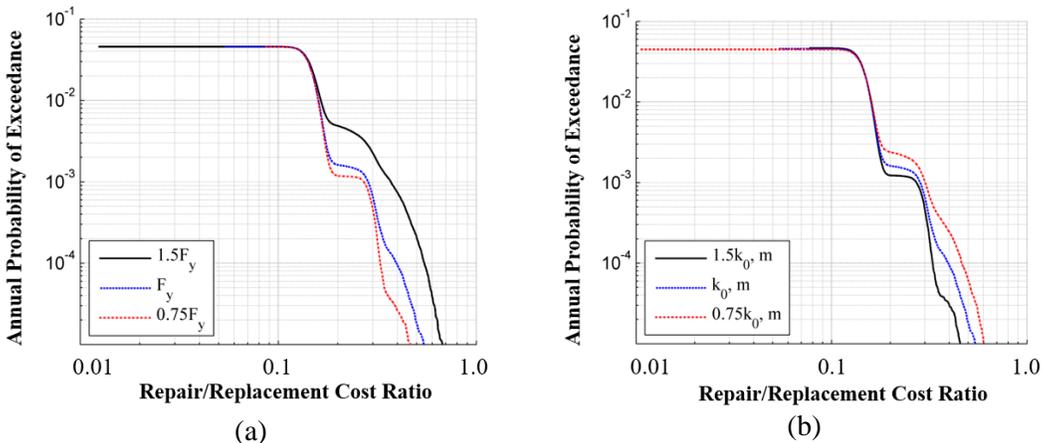
Figure 13: Probabilistic seismic loss hazard curves for SDOF systems with (a) different yield strengths, and (b) different initial stiffnesses

5 Inverse PBEE analysis using the PPBOSD framework

5.1 Inverse PBEE problem

The aforementioned inverse PBEE problem, i.e., achieving a probabilistic performance objective, is highly challenging as the design objective is probabilistic and defined based on the loss hazard (i.e., result of the last step of the forward PBEE analysis). As such, this design or inverse PBEE problem can be solved using the PPBOSD framework newly proposed in this paper.

For validation purposes, a well-posed inverse PBEE problem needs to be set up such that the solution to this problem is known as a priori. Thus, the target loss hazard is defined as the probabilistic loss hazard, $v_{L_T}^{Obj} = v_{L_T}(k_0^*, F_y^*)$, corresponding to a set of a priori selected optimum design parameters (e.g., $k_0^* = 137,200\,\text{kN/m}$, $F_y^* = 10,290\,\text{kN}$). The mathematical formulation for the optimization problem is defined in Eq. (14),

$$\underset{\{k_0, F_y\}}{Minimize}\ f(k_0, F_y) = \|v_{L_T}(k_0, F_y) - v_{L_T}^{Obj}\|_2^2$$

$$subject\ to:$$
$$80,000 \le k_0 \le 187,200\ \ (\text{kN/m})$$
$$6,290 \le F_y \le 15,290\ (kN)$$

$$(14)$$

where the implicit objective function $f(k_0, F_y)$ defines the discrepancy between the current loss hazard curve $v_{L_T}(k_0, F_y)$ and the target loss hazard curve $v_{L_T}^{Obj}$, e.g., measured by the sum square regression/error (SSR) or L-2 norm square $\left(\|...\|_2^2\right)$. The objective function defined here is based on the total loss hazard curve, which involves a complicated implicit function evaluated through executing the simulator (e.g., the finite element model of the structure of interest subject to an ensemble of earthquake excitations) and evaluating performance objectives (e.g., the forward PBEE analysis). The proposed PPBOSD framework is expected, by using as a starting point an arbitrary but reasonable initial design, e.g., $k_0 = 100,000\,\text{kN/m}$, $F_y = 14,000\,\text{kN}$), to steer the design process such that the loss hazard curve gets as close as possible to the target loss hazard curve and, in this validation example, to recover the optimum design parameters which are known a priori. The validation problem for the proposed PPBOSD framework is illustrated in Fig. 14. Note that in this validation case, the optimum parameters are selected a priori with the corresponding loss hazard curve taken as the target loss hazard curve. However, in a regular (real-world) problem, the optimum design is not known in advance and instead is expected to be determined using the PPBOSD framework presented here.
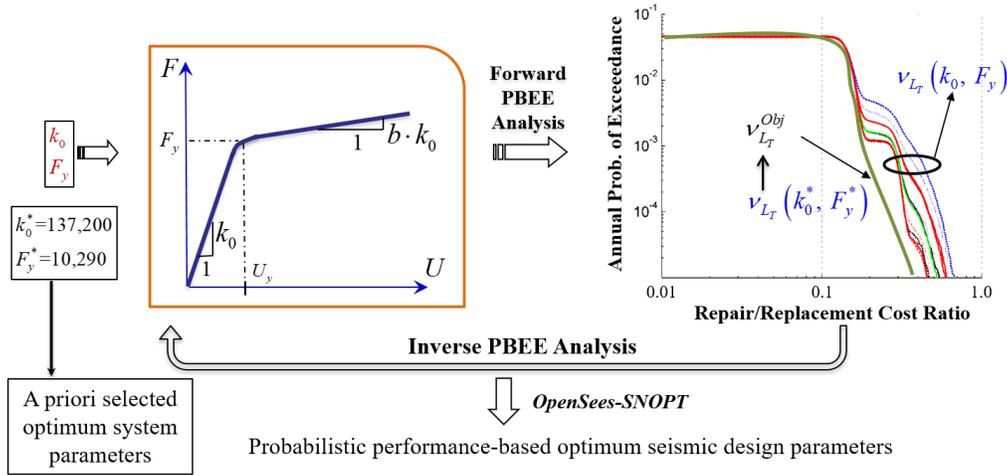
Figure 14: Illustration of validation problem for the proposed PPBOSD framework

5.2 Solution to the inverse PBEE problem

In the PPBOSD framework, tuning the initial design parameters requires computer-aided adjustment in an iterative way through mathematical optimization. Different optimization algorithms can be integrated in the PPBOSD framework, but this issue is beyond the scope of this study. Instead, the sparse nonlinear optimization software SNOPT, which was linked with *OpenSees* into the extended framework denoted as *OpenSees-SNOPT* [Gu, Barbato, Conte et al. (2012)], is used in the current version of the PPBOSD framework. For the validation example considered here, gradient-based sequential-quadratic programming (SQP) algorithms in *SNOPT* are used to tune the system parameters for a SDOF structural bridge model optimally rated for the target loss hazard curve.

The optimization process (which stopped when the relative reduction in the objective function value was less than 1.0×10^{-5}) and results are summarized in Fig. 15, including the iteration path over the plot of the objective function (both the (3D) surface plot and the contour plot). The optimum solution $\mathbf{X}^{end}$ obtained by the PPBOSD framework ($k_0^{end}=135{,}774$ kN/m, $F_y^{end}=10{,}038$ kN) is close to the true optimum design point ($k_0^*=137{,}200$ kN/m, $F_y^*=10{,}290$ kN) with an error of 1.0% for the initial stiffness and 2.4% for the yield strength. The evolutions of the demand hazard and loss hazard curves during the optimization process are shown in Fig. 16. It is observed that over six iterations, both the loss hazard and demand hazard curves are driven closer and closer to their respective target hazard curves corresponding to the a priori selected optimum design parameters. Thus, the proof-of-concept example presented successfully illustrates and validates the proposed PPBOSD framework.

The proposed PPBOSD framework is expected to be applied to more complex real-world problems in the field of earthquake engineering, and to support the decision-making process in structural design/retrofit with probabilistic performance objectives highly pertinent to the various stakeholders. Note that the illustrative example considers the

continuous range of hazard levels, while in practice, a finite (small) set of discrete hazard levels can be used to define practical probabilistic performance objectives, e.g., focusing on a low hazard level and a high hazard level. Additionally, the objective functions of the optimization problems solved using the PPBOSD framework can also be defined in terms of the conditional demand hazard, unconditional demand hazard, and damage hazard, instead of the loss hazard exemplified in this paper.
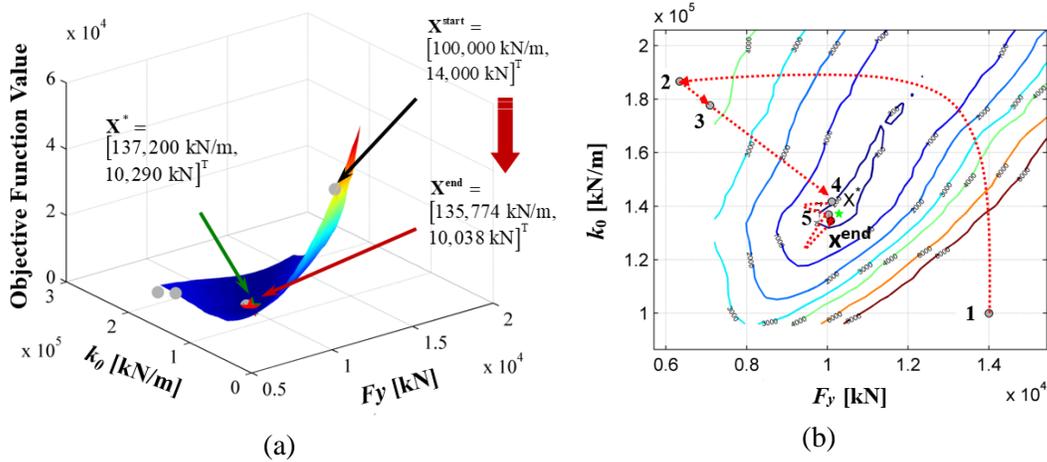
Figure 15: Optimization path for the PPBOSD illustrative example: (a) 3D plot, and (b) contour plot of the objective function
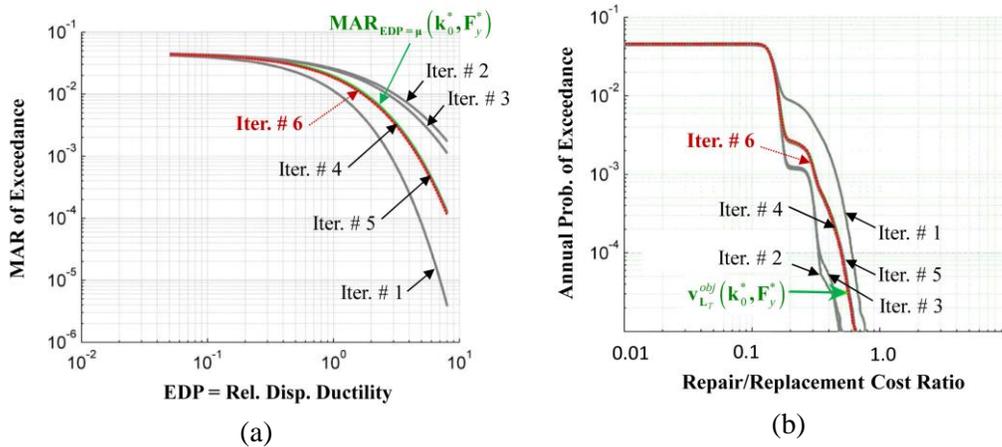
Figure 16: Evolution of the PBEE evaluation results during the optimization process: (a) probabilistic seismic demand hazard curves, and (b) probabilistic seismic loss hazard curves

6 Conclusions and discussion

The well-established probabilistic performance-based earthquake engineering (PBEE) methodology has been mainly used for performance evaluation of existing or newly designed structural, geotechnical or soil-foundation-structural systems, thus referred to

herein as forward PBEE analysis. In contrast, the use of the PBEE methodology for design purposes in the presence of uncertainty is more limited, because design is strictly a more challenging inverse PBEE analysis problem. To address the performance-based design issue, this paper proposes a probabilistic performance-based optimum seismic design (PPBOSD) framework as an extension to the existing PBEE assessment methodology. In the PPBOSD framework, a decision layer supported by computational optimization is wrapped around the forward PBEE analysis methodology, which is aimed to tune the design parameters of the civil infrastructure system of interest to achieve seismic performance objectives expressed in probabilistic terms. As a first step of promoting the proposed PPBOSD framework, this paper focuses on illustrating and validating the framework using a simple proof-of-concept example, i.e., a nonlinear inelastic SDOF model representing macroscopically the longitudinal or transverse behavior of a bridge structure with a priori selected optimum design parameters. The PPBOSD framework in conjunction with the combined structural modeling and optimization software OpenSees-SNOPT successfully recovered the a priori selected optimum design parameters from a set of initial parameter values purposely taken away from the optimum values. It shows that a complicated and implicit probabilistic performance objective (e.g., defined in terms of a targeted probabilistic loss hazard curve) can be achieved using the PPBOSD framework. Note that the illustrative example used in this paper is based on a simple macroscopic structural model with two primary design variables for the purpose of clearly demonstrating the concepts and procedure. However, the design of complex real-world civil infrastructure systems (with more design variables) can also utilize the proposed PPBOSD framework, with the computational cost issue appropriately addressed (e.g., by using cloud and/or high-performance computing).

However, when applying the proposed PPBOSD framework to real-world structures, the following potential difficulties or limitations will need to be addressed in future research. (1) A numerically robust nonlinear model of the real-world structure is required. Non-collapse related non-convergence issues during the seismic response analysis need to be resolved using, for example, adaptive switching between nonlinear solution algorithms, integration methods, convergence criteria, etc., or explicit integration. If a physical collapse related convergence issue occurs, the collapse probability needs to be considered in the overall methodology [Zhang (2006); Romano, Faggella, Gigliotti et al. (2018)]. However, distinguishing between lack of convergence due to numerical issues or due to imminent physical failure (collapse) of the structure being analyzed is challenging and can possibly be addressed by artificial intelligence. (2) To render the PBEE analysis and the PPBOSD more practical, fragility curves for various structural members as well as the associated repair/replacement costs need to be developed and compiled for various types of structures as in the FEMA P-58 PACT tool [FEMA (2012)] for buildings. (3) The gradient-based optimization algorithms currently available in OpenSees-SNOPT may lead to a local minimum, and this issue can be addressed by using multiple starting points or using other global optimization methods. It is worth noting that from a practical viewpoint, a local minimum could already be highly beneficial, representing a significant improvement over the initial design. All the challenging issues mentioned above and possibly others can be appropriately tackled and implemented in the versatile architecture of the proposed framework.

The probabilistic design objective is expressed in terms of the target loss hazard curve in this study, but it can be defined to closely reflect the design objectives of decision-makers in practice. More importantly, this framework provides the proper tool needed to develop, calibrate and validate simplified probabilistic performance-based design procedures for engineering practice. Finally, the proposed PPBOSD framework can be extended to other natural and man-made hazards (e.g., tsunami, wind/hurricane/tornadoes, storm surge, fire, blast), as well as multi-hazard design problems.

References

Austin, M.; Pister, K.; Mahin S. A. (1987): Probabilistic design of moment-resistant frames under seismic loading. *Journal of Structural Engineering*, vol. 113, no. 8, pp. 1660-1677.

Baker, J. W. (2005): *Vector-Valued Ground Motion Intensity Measures for Probabilistic Seismic Demand Analysis* (*Ph.D. Thesis)*. Stanford University, California.

Baker, J. W. (2007): Probabilistic structural response assessment using vector-valued intensity measures. *Earthquake Engineering and Structural Dynamics*, vol. 36, no. 13, pp. 1861-1883.

Barbato, M.; Tubaldi, E. (2013): A probabilistic performance-based approach for mitigating the seismic pounding risk between adjacent buildings. *Earthquake Engineering and Structural Dynamics*, vol. 42, no. 8, pp. 1203-1219.

Comerio, M. C.; Stallmeyer, J. C.; Smith, R.; Makris, N.; Konstantinidis, D. et al. (2005): PEER testbed study on a laboratory building: exercising seismic performance assessment. *PEER Report No. PEER 2005/12*. Pacific Earthquake Engineering Research (PEER) Center, Oakland, California.

Conte, J. P.; Zhang, Y. (2007): Performance-based earthquake engineering: application to an actual bridge-foundation-ground system. *Proceedings of the 12th Italian National Conference in Earthquake Engineering*.

Cornell, C. A. (1968): Engineering seismic risk analysis. *Bulletin of the Seismological Society of America*, vol. 58, no. 5, pp. 1583-1606.

Cornell, C.; Krawinkler, H. (2000): Progress and challenges in seismic performance. *PEER Center News*, vol. 3, no. 2.

Eguchi, R. T.; Goltz, J. D.; Taylor, C. E.; Chang, S. E.; Flores, P. J. et al. (1998): Direct economic losses in the Northridge earthquake: a three-year post-event perspective. *Earthquake Spectra*, vol. 14, no. 2, pp. 245-264.

Ellingwood, B. R. (2000): LRFD: implementing structural reliability in professional practice. *Engineering Structures*, vol. 22, no. 2, pp. 106-115.

Federal Emergency Management Agency (FEMA) (2012): Seismic performance assessment of buildings volume 1-methodology. *Technical Report FEMA-P58*, Washington, DC.

Gardoni, P.; Mosalam, K. M.; Der Kiureghian, A. (2002): Probabilistic capacity models and fragility estimates for reinforced concrete columns based on experimental observations. *Journal of Engineering Mechanics*, vol. 128, no. 10, pp. 1024-1038.

Goulet, C. A.; Haselton, C. B.; Mitrani-Reiser, J.; Beck, J. L.; Deierlein, G. G. et al. (2007): Evaluation of the seismic performance of a code-conforming reinforced concrete frame building - from seismic hazard to collapse safety and economic losses. *Earthquake Engineering and Structural Dynamics*, vol. 36, no. 13, pp. 1973-1997.

Gu, Q.; Barbato, M.; Conte, J. P.; Gill, P. E. (2012): OpenSees-SNOPT framework for finite-element-based optimization of structural and geotechnical systems. *Journal of Structural Engineering*, vol. 137, no. 6, pp. 822-834.

Günay, S.; Mosalam, K. M. (2013): PEER performance-based earthquake engineering methodology revisited. *Journal of Earthquake Engineering*, vol. 17, no. 6, pp. 829-858.

Haselton, C. B.; Liel, A. B.; Deierlein, G. G.; Dean, B. S.; Chou, J. H. (2011): Seismic collapse safety of reinforced concrete buildings: I. Assessment of ductile moment frames. *Journal of Structural Engineering*, vol. 137, no. 4, pp. 481-491.

Haukaas, T. (2008): Unified reliability and design optimization for earthquake engineering. *Probabilistic Engineering Mechanics*, vol. 23, no. 4, pp. 471-481.

Jalayer, F.; Cornell, A. (2003): *A Technical Framework for Probability-Based Demand and Capacity Factor (DCFD) Seismic Formats*. RMS Technical Report No.43 to the PEER Center, Stanford University, California.

Jensen, H. A.; Valdebenito, M. A.; Schuëller, G. I.; Kusanovic, D. S. (2009): Reliability-based optimization of stochastic systems using line search. *Computer Methods in Applied Mechanics and Engineering*, vol. 198, no. 49, pp. 3915-3924.

Kunnath, S. K.; Larson, L.; Miranda, E. (2006): Modeling considerations in probabilistic performance-based seismic evaluation: case study of the I-880 viaduct. *Earthquake Engineering and Structural Dynamics*, vol. 35, no. 1, pp. 57-75.

Li, Y. (2014): *Probabilistic Performance-Based Optimum Seismic Design of Seismic Isolation for California High-Speed Rail Prototype Bridge (Ph.D. Thesis)*. University of California, San Diego, California.

Li, Y.; Conte, J. P. (2017): Probabilistic performance-based optimum design of seismic isolation for a California high-speed rail prototype bridge. *Earthquake Engineering and Structural Dynamics*, vol. 47, no. 2, pp. 497-514.

Li, Y.; Conte, J. P. (2019): Probabilistic evaluation of seismic isolation effects for a California high-speed rail prototype bridge. *Journal of Structural Engineering*.

Lin, T.; Haselton, C. B.; Baker, J. W. (2013): Conditional-spectrum-based ground motion selection. part I: hazard consistency for risk-based assessments. *Earthquake Engineering and Structural Dynamics*, vol. 42, no. 12, pp. 1847-1865.

Liu, P. L.; Der Kiureghian, A. (1986): Multivariate distribution models with prescribed marginals and covariance's. *Probabilistic Engineering Mechanics*, vol. 1, no. 2, pp. 105-112.

Luco, N.; Cornell, C. A. (2007): Structure-specific scalar intensity measures for near-source and ordinary earthquake ground motions. *Earthquake Spectra*, vol. 23, no. 2, pp. 357-392.

Mackie, K. R.; Stojadinović, B. (2007): Performance-based seismic bridge design for damage and loss limit-states. *Earthquake Engineering and Structural Dynamics*, vol. 36, no. 13, pp. 1953-1971.

Mosalam, K. M.; Günay, S. (2014): Seismic performance evaluation of high voltage disconnect switches using real-time hybrid simulation: I. System development and validation. *Earthquake Engineering & Structural Dynamics*, vol. 43, no. 8, pp. 1205-1222.

Petersen, M. D.; Frankel, A. D.; Harmsen, S. C.; Mueller, C. S.; Haller, K. M. et al. (2008): *Documentation for the 2008 Update of the United States National Seismic Hazard Maps*. U.S. Geological Survey Open-File Report, California.

Porter, K. A. (2003): An overview of PEER's performance-based earthquake engineering methodology. *Proceedings of Conference on Applications of Statistics and Probability in Civil Engineering*, Civil Engineering Risk and Reliability Association (CERRA), San Francisco, California.

Porter, K. A.; Beck, J. L.; Shaikhutdinov, R. V. (2002): Sensitivity of building loss estimates to major uncertain variables. *Earthquake Spectra*, vol. 18, no. 4, pp. 719-743.

Romano, F.; Faggella, M.; Gigliotti, R.; Zucconi, M.; Ferracuti, B. (2018): Comparative seismic loss analysis of an existing non-ductile RC building based on element fragility functions proposals. *Engineering Structures*, vol. 177, pp. 707-723.

Shome, N.; Cornell, C. A.; Bazzurro, P.; Carballo, J. E. (1998): Earthquakes, records, and nonlinear responses. *Earthquake Spectra*, vol. 14, no. 3, pp. 469-500.

Taflanidis, A. A.; Beck, J. L. (2009): Stochastic subset optimization for reliability optimization and sensitivity analysis in system design. *Computers & Structures*, vol. 87, no. 5-6, pp. 318-331.

Tubaldi, E.; Barbato, M.; Dall'Asta, A. (2016): Efficient approach for the reliability-based design of linear damping devices for seismic protection of buildings. *ASCE-ASME Journal of Risk and Uncertainty in Engineering Systems, Part A: Civil Engineering*, vol. 2, no. 2, pp. C4015009.1-C4015009.10.

Yang, T. Y.; Moehle, B.; Stojadinovic, B.; Der Kiureghian, A. (2009): Seismic performance evaluation of facilities: methodology and implementation. *Journal of Structural Engineering*, vol. 135, no. 10, pp. 1146-1154.

Zakeri, B.; Zareian, F. (2017): Bridge design framework for target seismic loss. *Journal of Bridge Engineering*, vol. 22, no. 10, pp. 04017061-1-04017061-15.

Zhang, Y. (2006): *Probabilistic Structural Seismic Performance Assessment Methodology and Application to an Actual Bridge-Foundation-Ground System (Ph.D. Thesis).* University of California, San Diego, California.